Frontiers in
BIOMEDICAL TECHNOLOGIES
August 2014, Volume 1, Number 3

Quantification of PET and CT Misalignment Errors Due to Bulk Motion in Cardiac PET/CT Imaging: Phantom and Clinical Studies

Pardis Ghafarian[1,2], Mohammad Reza Ay[3,4], Armaghan Fard-Esfahani[5], Arman Rahmim[6], Habib Zaidi[7,8,9*]

1. Chronic Respiratory Diseases Research Center, National Research Institute of Tuberculosis and Lung Diseases (NRITLD), Shahid Behesht University of Medical Sciences, Tehran, Iran.
2. PET/CT and Cyclotron Center, Masih Daneshvari Hospital, Shahid Beheshti University of Medical Sciences, Tehran, Iran.
3. Research Center for Molecular and Cellular Imaging, Tehran University of Medical Sciences, Tehran, Iran.
4. Department of Medical Physics and Biomedical Engineering, Tehran University of Medical Sciences, Tehran, Iran.
5. Research Center for Nuclear Medicine, Tehran University of Medical Sciences, Tehran, Iran.
6. Department of Radiology, Johns Hopkins University, Baltimore, Maryland, USA.
7. Division of Nuclear Medicine and Molecular Imaging, Geneva University Hospital, CH-1211 Geneva, Switzerland.
8. Geneva Neuroscience Center, Geneva University, CH-1205 Geneva, Switzerland.
9. Department of Nuclear Medicine and Molecular Imaging, University of Groningen, University Medical Center Groningen, Groningen, Netherlands.

Received: May 15 2014
Accepted: July 11 2014

ABSTRACT

Purpose: Non simultaneous acquisition between CT and PET module can introduce misalignment artefact in cardiac PET/CT imaging due to patient motion. We assessed the clinical impact of patient motion and the resulting mismatch between CT and corresponding CT-based attenuation corrected (CTAC) PET images on apparent myocardial uptake values in cardiac PET/CT imaging.

Methods: The evaluation of patient motion was performed using clinical and experimental phantom studies acquired on the Biograph TP 64 PET/CT scanner. In order to simulate patient motion, CT images were manually shifted from 0 to 20 mm in steps of 5-mm in six different directions. The reconstructed PET images using shifted CT were compared with the original PET images. The assessment of PET images was performed through qualitative interpretation by an experienced nuclear medicine physician and through quantitative analysis using volume of interest based analysis. Moreover, Box and Whisker plots were calculated and bull's eye view analysis performed. PET images were also reoriented along the short, horizontal and vertical long axis views for a better qualitative interpretation.

Results: A 20-mm shift in the right direction between attenuation and PET emission scans produced mean absolute percentage difference in uptake values in the lateroanterior (33.42±9.07) and lateroinferior (27.39±10.43) segments of the myocardium.

Conclusion: Misalignment could introduce artifactual nonuniformities in apparent myocardial uptake value and the variations were more significant for the misalignment toward the right, feet and head directions, in such a way that even with a 5-mm shift in the CT image, errors in interpretation of PET images could occur. Furthermore, errors in PET uptake estimates were observed for movements as large as 10-mm in the left, posterior and anterior directions.

Keywords:
Cardiac PET/CT, Misalignment Artefacts, Attenuation Correction, Image Registration.

**** Corresponding Author:***
Habib Zaidi, PhD
Geneva University Hospital, Division of Nuclear Medicine and Molecular Imaging, CH-1211 Geneva, Switzerland.
Tel:+41 22 372 7258 / Fax: +41 22 372 7169
E-mail: habib.zaidi@hcuge.ch

1. Introduction

With the advent of PET/CT systems equipped with 64/128 slices CT scanner, full cardiac assessment such as evaluation of calcium score, myocardial blood flow at rest and during pharmacologic stress in long with CT coronary angiography, was made possible in one imaging session [1, 2]. This method definitely causes improvement in the diagnostic accuracy and patient comfort [3-6]. Various strategies were proposed to reduce the number of CT imaging sessions in cardiac PET/CT to decrease patient dose in multimodality cardiovascular imaging [7, 8]. Misaligned attenuation correction including respiratory and global motion leads to artifactual errors in quantitative analysis in cardiac PET/CT images due to CT data are used as the attenuation map. In addition to respiratory artefacts in cardiac PET/CT imaging, the metallic leads from ICD and pacemaker can produce serious errors in myocardial wall uptake [9, 10]. Misregistration due to temporal resolutions and respiratory patterns between PET and CT data can generate inaccuracies in tracer uptake value in the thorax region [11] and can introduce moderate to severe errors in cardiac PET/CT imaging [12]. Various groups introduced different approaches to decrease these artefacts [13-15]. Pan et al. [16] proposed a method based on respiratory-averaged CT to minimize the white band artefact in the lower thorax of PET images, however, Alessio et al. [17] found that acquiring cine CT can introduce to acceptable alignment between CT and PET data. Since the heart is surrounded by the lung and diaphragmatic regions with different attenuation factors, global patient motion between two scanners can produce serious artefact in myocardial wall obtained with 13N-ammonia, or 18F-FDG due to CT-based attenuation corrected (CTAC) PET images. The aim of the present study is to quantitatively evaluate the effect of patient motion between PET and CT data acquisition on tracer uptake in myocardial PET imaging using CTAC of PET data in both experimental phantoms and clinical studies.

2. Methods

2.1. Experimental Phantom Study

The RSD thorax phantom (Radiology Support Devices, Long Beach, CA) was used to evaluate the net effect of global patient movement between CT and PET data through the elimination of potential cardiac and respiratory motion. The RSD thorax phantom is a tissue equivalent anthropomorphic phantom designed from patient data and is suitable to assess the extent and severity of myocardial defects in male and female patients. The RSD heart model is based on vacuum-formed shells obtained from high resolution, contrast-enhanced and ultrafast CT images of a normal human that is somewhat simplified for practicality. The volume of the heart chamber is 284 ml while the volume of the myocardial wall is 240 ml. To model the typical biodistribution of 370 MBq of FDG in a normal subject, the activity distribution in individual organs of the RSD thorax phantom were as follows: thorax cavity (43.460 MBq), myocardial wall (5.712MBq), left lung (1.221 MBq), right lung (1.739 MBq) and liver(12.446 MBq) [18]. The RSD phantom was scanned using the same protocol employed for routine clinical studies.

2.2. Clinical Studies

Three patient studies including one 13N-ammonia perfusion and two 18F-FDG PET/CT viability examinations were used in this study. The patients positioned in the scanner with arms behind their head. For each18F-FDG study, a low-dose CT scan (120 kVp, 74 effective mAs, 24×1.2 collimation, 0.45:1 pitch, 1 sec revolution time) with regular shallow breathing was obtained prior to PET emission data acquisition. Subsequently, PET data were acquired for one bed position in list-mode format for 10 minutes. For 13N-ammonia perfusion imaging, after injection of an intravenous dipyridamole stress, a low-dose CT scan (same parameters as above) was performed. Thereafter, the stress examination was acquired (12 min) in list-mode format. The rest study was performed after 20 min following a second injection of 13N-ammonia followed by a second low-dose CT.

2.3. PET/CT Data Acquisition and Reconstruction

Clinical and experimental phantom studies were performed on the Biograph TP 64 PET/CT scanner (Siemens Medical Solutions, Erlangen, Germany), equipped with volumetric CT to advance cardiovascular imaging capabilities. The PET scanner is comprised of 39 rings with a total of 24336 LSO crystals of dimensions 4×4×25 mm operating in a fully three-dimensional mode with an axial field-of-view (FOV) of 162 mm. The CT sub-system is comprised of a 40-row ceramic detector with 1344 channels per row and adaptive collimation. The CT module operates with the z-sharp technique to acquire 64 slices per rotation.

To evaluate the influence of misalignment between CT and PET images on the myocardial uptake values, CT images of both the RSD phantom and clinical studies were manually shifted in six different directions includ-

Table 1. Evaluation of misalignment between ACCT and emission corresponding data for all patients in this study.

Examination	X (cm)	Y (cm)	Z (cm)	XY (°)	XZ (°)	YZ (°)
Patient 1V	**-0.207**	-0.356	0.061	0.349	0.539	0.042
Patient2V	**-0.099**	-0.307	0.295	-0.404	0.357	-0.121
Patient 3S	**0.587**	-0.683	0.221	0.043	0.395	-0.163
Patient 3R	**-0.516**	-0.208	0.432	0.094	0.579	-0.213

X, Y, Z translation in the x, y, z direction.

XY, XZ, YZ rotation in the xy, xz, yz planes.

ACCT, attenuation correction computed tomography;

R, rest mode in perfusion examination; S, stress mode in perfusion examination; V, viability examination

ing left, right, feet, head, anterior and posterior, from 0 to 20 mm in steps of 5 mm. The resampled CT data were, then, used for attenuation correction of PET images. The list-mode PET data were rebinned into 2-D sinograms and corrections for detector sensitivity, randoms, dead-time, scatter and attenuation were applied. An ordered-subset expectation maximization (OSEM) algorithm was applied (6 iterations and 8 subsets) with a 5-mm FWHM Gaussian post-smoothing, a zoom factor of 2 and a 256×256 image matrix. Subsequently, 25 datasets were obtained for each PET acquisition including one PET image attenuation corrected with the aligned CT and 24 PET images attenuation corrected with shifted CT images. It should be noted that the perfusion protocol employed in our department requires two separate CT scans for attenuation correction of the stress and rest PET emission scans. Therefore, 50 PET datasets were obtained for quantitative evaluation of misalignment artefacts.

2.4. Assessment Strategy

In patient study, the misalignment between attenuation correction computed tomography (ACCT) and corresponding emission data was quantified using both the commercial coregistration package provided in the HERMES multimodality fusion software (Hermes Medical Solutions, Stockholm, Sweden), and the qualitative visual assessment performed by a qualified nuclear medicine physician. So the alignment between CT and PET data were proved, the manual misalignment were investigated by shifted CT in different directions. CT-based attenuation corrected of PET images using aligned and shifted CT data were evaluated using both qualitative interpretation and quantitative analysis. 500 volumes of interest (VOIs) were delineated on each PET images using the AMIDE image processing software on myocardial segments of the left ventricle [19]. Linear regression analysis of pairs of PET data corrected for attenuation using aligned and shifted CT images enables the derivation of Pearson correlation coefficients (R2) and slopes was performed. Box and Whisker plots and semi-quantitative analysis of uptake values based on 17-segment bull's eye view model (each segment normalized to the maximum value) were performed as well. The mean absolute percentage difference of tracer uptake in all segments in the myocardial wall was also evaluated.

Table 2. Summary of correlation coefficients/slopes of regression lines resulting from VOI-based analysis in the myocardial wall (n=500)of PET images corrected for attenuation using aligned vs. shifted CT for two clinical studies. Shifts were introduced only in three directions.

Study	Correlation Coefficient/Slope Posterior Head Right				P value
	5 mm	10 mm	15 mm	20 mm	
Patient V	0.95/0.91 0.95/0.98 0.97/0.88	0.84/0.81 0.83/0.97 0.87/0.74	0.47/0.59 0.69/0.96 0.61/0.59	0.22/0.42 0.57/0.95 0.30/0.43	<0.0001
Patient S	0.95/0.95 0.93/0.92 0.92/0.96	0.68/0.82 0.78/0.84 0.68/0.82	0.68/0.82 0.78/0.84 0.68/0.82	0.17/0.48 0.49/0.69 0.15/0.42	<0.0001
Patient R	0.96/1.03 0.93/0.93 0.88/0.96	0.81/1.01 0.79/0.85 0.58/0.84	0.66/0.94 0.64/0.77 0.23/0.65	0.41/0.79 0.51/0.70 0.10/0.48	<0.0001

R: rest mode in perfusion study; S: stress mode in perfusion study; V: viability study

PET images were also reoriented along the short axis and horizontal/vertical long axis views for clinical interpretation by an experienced nuclear medicine physician.

Uptake values in pairs of PET images corrected for attenuation using aligned and shifted CT data were also compared using a two-sided paired t-test. Statistical analysis was evaluated using the SPSS software (SPSS Inc., Chicago, Illinois, USA, version 16). P-values less than 0.05 were considered statistically significant.

3. Results

Figure 1(a-d) illustrate the correlation plot between PET data corrected for attenuation using shifted CT in the right direction (from 0 to 20 mm in steps of 5 mm) and aligned CT for the viability protocol using the RSD phantom. 500 VOIs were used for the calculation of the correlation plot for each PET dataset in all segments of the myocardial wall. As expected, the slope of the regression line decreases when the misalignment between CT and PET data increases.

Table 3. Mean absolute percentage difference in tracer uptake for clinical studies in the myocardial wall through bull's eye view between PET images corrected for attenuation without and with shifted CT images in different directions.

Mean absolute percentage difference in tracer uptake (mean±SD)						
Myocardial wall	Anterior Head Left			Posterior Feet Right		
	5 mm	10 mm	20 mm	5 mm	10 mm	20 mm
Anteroseptal	1.17±0.91 2.08±1.80 0.71±0.18	1.60±1.09 4.64±3.71 4.42±3.20	2.33±1.24 8.60±7.30 8.50±4.74	1.98±1.83 3.89±2.94 2.92±1.21	4.22±2.10 12.89±5.78 6.60±3.63	12.66±8.52 23.55±9.92 11.32±9.90
Anterolateral	1.98±0.72 1.24±1.05 3.05±1.91	2.83±2.39 2.16±1.68 4.64±3.35	2.40±1.11 6.30±4.08 5.71±3.40	1.84±1.07 1.12±1.00 4.83±3.95	4.56±3.66 6.05±4.00 11.44±8.43	15.27±12.17 14.76±10.52 21.28±14.03
Lateroanterior	1.88±1.03 5.70±2.55 5.10±2.55	3.14±2.83 12.81±5.25 7.34±4.03	4.74±3.01 29.03±8.77 9.61±8.19	2.80±1.68 5.43±2.16 7.40±3.43	3.50±3.26 6.54±3.78 16.96±7.50	5.30±2.43 11.48±7.44 33.42±9.07
Lateroinferior	2.08±1.18 7.34±3.23 4.61±2.78	3.49±1.88 15.99±5.63 6.59±4.53	7.70±3.33 32.96±9.74 9.70±6.45	4.03±2.88 7.67±3.25 5.47±3.18	4.88±4.04 10.01±4.76 11.99±7.15	9.18±5.63 13.48±8.89 27.39±10.43
Inferolateral	1.32±1.09 3.50±2.72 1.62±0.74	4.24±3.59 8.11±4.23 2.75±1.88	10.88±8.64 16.63±7.32 5.83±3.55	3.47±2.15 5.00±2.96 1.79±0.71	5.33±5.16 6.16±5.54 3.92±2.81	10.03±5.44 13.31±7.93 5.81±3.26
Inferoseptal	1.10±0.66 1.52±1.01 1.32±0.62	2.68±2.12 4.41±3.51 4.54±2.88	6.93±6.37 9.27±6.03 8.91±6.03	1.94±1.16 2.46±2.17 2.78±1.84	2.42±1.82 3.22±2.93 5.36±3.78	5.50±2.80 11.63±10.17 8.82±6.61
Septoinferior	1.09±0.22 1.65±0.94 2.34±1.20	1.81±1.32 2.21±1.39 5.28±2.64	4.56±2.07 4.53±2.69 11.32±5.49	2.55±1.50 1.06±0.71 2.95±1.52	3.18±3.11 5.15±4.46 5.53±4.01	6.01±3.44 15.86±12.26 10.78±6.85
Septoanterior	1.94±1.20 2.39±1.47 1.67±0.45	2.02±1.62 4.87±3.99 5.06±2.63	2.50±2.03 8.69±7.31 11.01±4.68	1.86±1.55 2.75±2.15 2.73±1.13	3.02±2.27 10.65±6.13 4.80±3.21	2.81±2.05 22.16±10.97 8.22±7.68
Apex	1.29±0.95 2.10±1.66 2.09±1.41	2.26±1.71 2.74±1.18 4.37±3.41	4.41±3.71 5.69±4.83 7.31±6.67	1.30±1.10 2.72±1.47 2.69±1.42	1.93±0.49 9.15±2.78 6.66±2.88	4.01±2.38 20.29±10.84 13.19±9.72

Table 1 summarizes the misalignment between ACCT and emission data as evaluated by rigid-body registration using the HERMES multimodality fusion software. As our aim is to evaluate the misalignment effect in uptake value of PET images, an understanding of the level of misalignment between these two CT and emission data makes sense for the purpose of this study. A low misalignment between these images guarantees reproducible and similar results when ACCT is shifted in different directions.

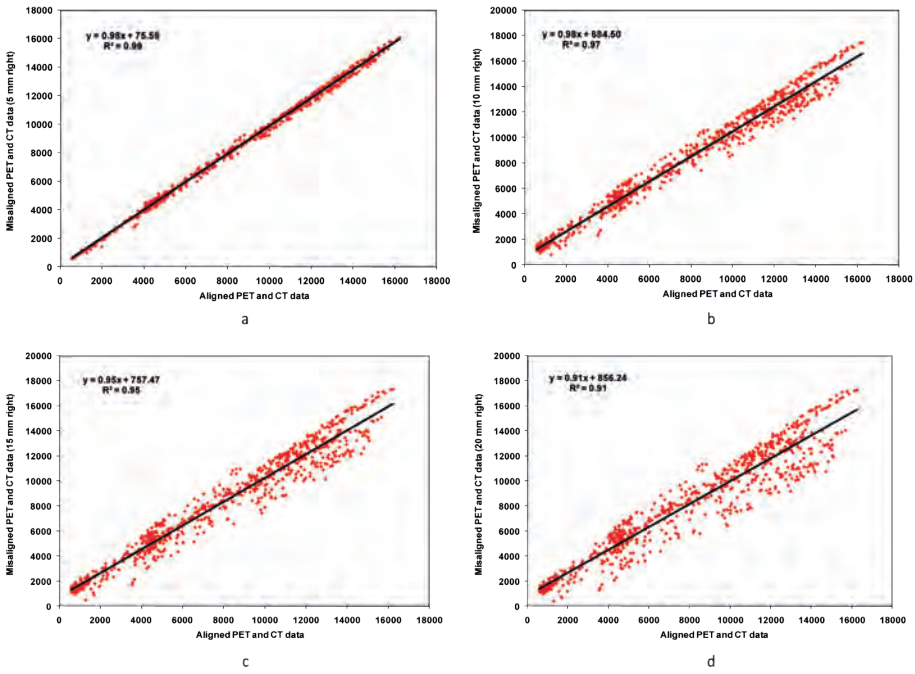

Figure 1. Correlation plots between PET images corrected for attenuation correction using the aligned and shifted CT to the right direction of the RSD phantom corresponding to: (a) 5 mm, (b) 10 mm, (c) 15 mm, and (d) 20 mm, (n=500, p<0.0001).

The correlation coefficients and slopes of the regression plots of PET images corrected for attenuation using CT images shifted in three directions and using different shifts were compared with PET images corrected with aligned CT for two clinical studies included in this work (table2). There is a higher correlation of the mean uptake values in the myocardial wall between PET images corrected for attenuation with 5 mm shift of the CT images in all directions (all value were not shown). However, both the correlation coefficient and the slope decrease when significant misalignments are introduced, especially in feet and right directions.

The percentage relative difference between reconstructed PET images using shifted CT vs. aligned CT for the RSD phantom and one clinical viability study are indicated by the Box and Whisker plots illustrated in figure 2. A large misalignment results in spread of boxes due to significant artificial uptake in the myocardial wall. The level of misalignment in anterior and posterior directions yields the smallest variation compared to other directions.

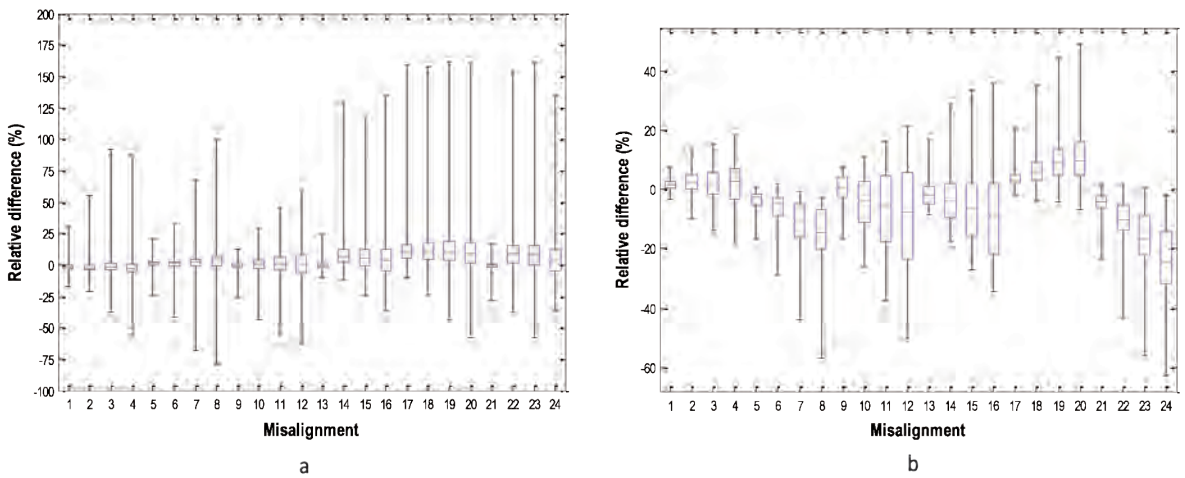

Figure 2. Box and Whisker plots illustrating the variation of percentage relative difference (maximum, upper quartile, median, lower quartile and minimum) resulting from the VOI-based analysis in the myocardial wall of PET images corrected for attenuation using shifted and aligned CT for: (a) the RSD phantom; (b) clinical viability study. (1-4 correspond to 5-20 mm shift anterior, 5-8 correspond to 5-20 mm shift posterior, 9-12 correspond to 5-20 mm shift head, 13-16 correspond to 5-20 mm shift feet, 17-20 correspond to 5-20 mm shift left, and 21-24 correspond to 5-20 mm shift right in steps of 5 mm).

Figures 3-4 demonstrate the influence of misalignment on the uptake value in the myocardial wall of PET images when using aligned CT vs. shifted CT in the right direction (5mm and 20mm, respectively). The visual assessment of PET images exhibit some artefacts in the anterior and lateral segments for a small misalignment expressed as large declines in the inferior and apex regions in large misalignments.

The mean absolute percentage difference of tracer uptake value in all myocardial segments based on the bull's eye view analysis of clinical studies (viability and perfusion examinations) are summarized in Table 3. A large misalignment can cause noticeable artefacts in most segments of the myocardial wall in different directions. It appears that erroneous uptake values in anterior and posterior directions are slightly less visible compared to other directions.

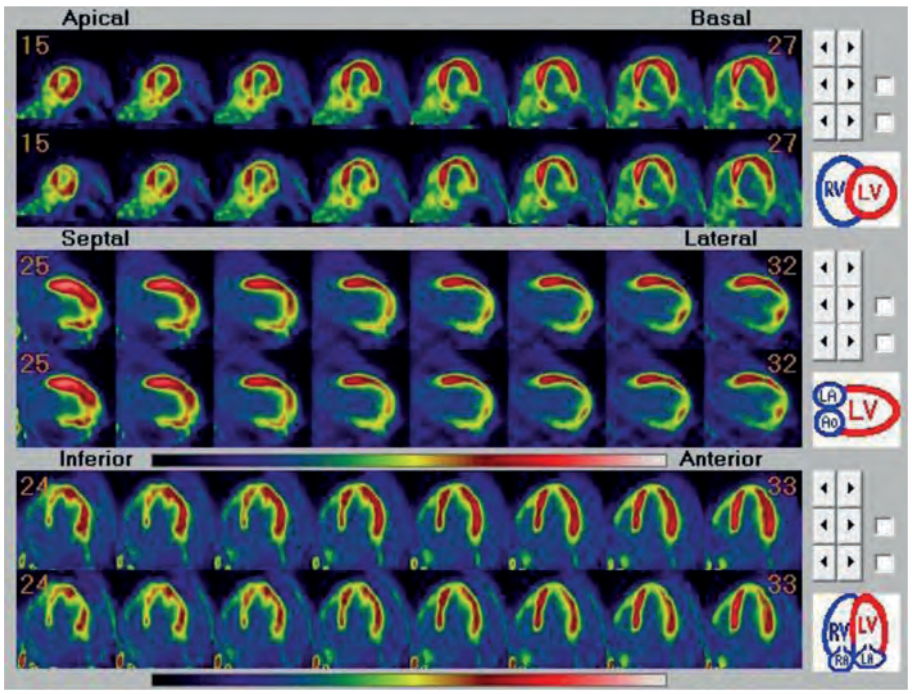

a

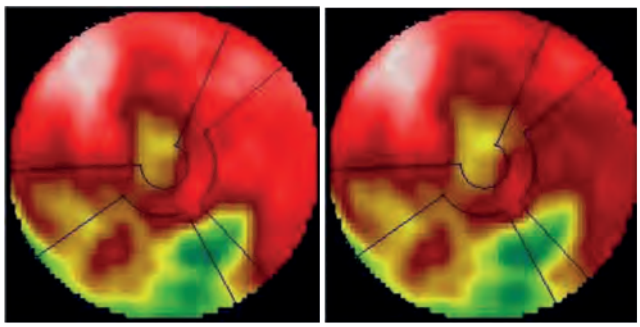

b

Figure 3. (a) Representation of typical short, vertical and horizontal long axis of a clinical stress perfusion PET study corrected for attenuation using: top row aligned CT and bottom row 5 mm shifted CT in the right direction. (b) Bull's eye view of the stress perfusion PET study corrected for attenuation using aligned CT (left) and 5 mm shifted CT in the right direction (right).

4. Discussion

In the present study, the global patient motion between CT and PET scanners based on experimental phantom and clinical study was assessed. Attenuation corrected PET images with misaligned CT can induce clinical misinterpretation due to project lung tissues onto the myocardial wall [20] or liver dome and part of the diaphragm in the thorax region. A 2-cm mismatch can introduce significant errors in the thorax region

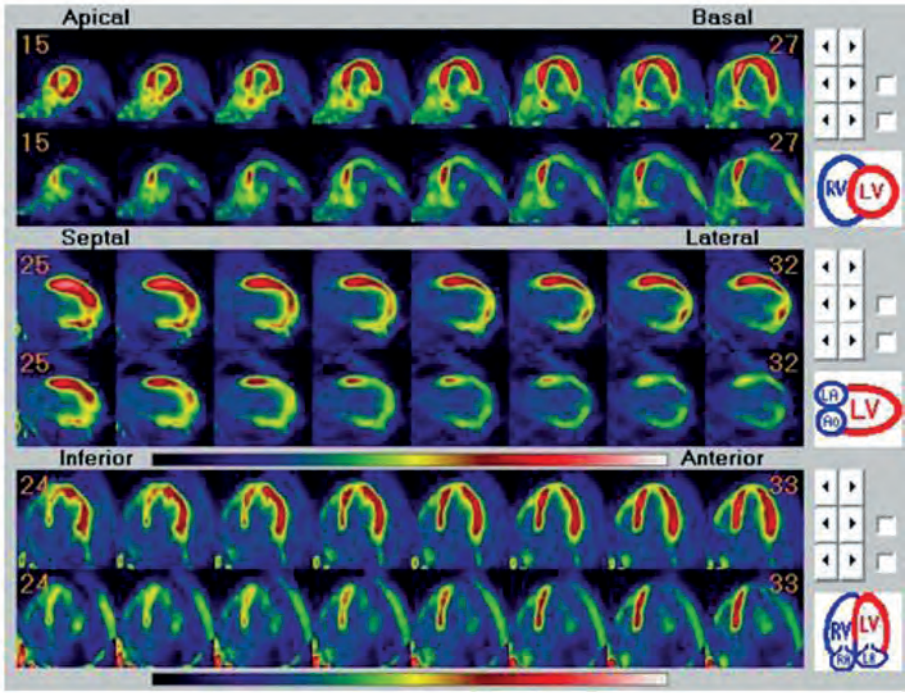

a

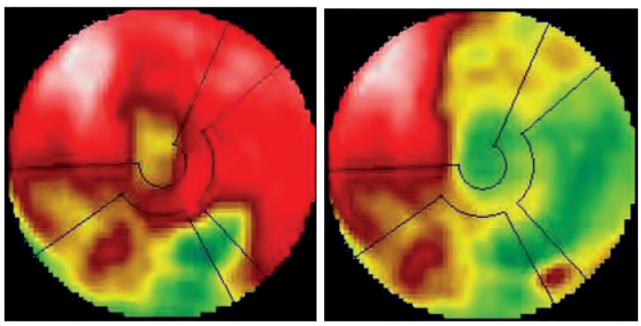

b

Figure 4. (a) Representation of typical short, vertical and horizontal long axis of a clinical stress perfusion PET study corrected for attenuation using: top row aligned CT and bottom row 20 mm shifted CT in the right direction. (b) Bull's eye view of the stress perfusion PET study corrected for attenuation using aligned CT (left) and 20 mm shifted CT in the right direction (right).

[21] which is similar to our findings. The VOI-based analysis of the PET data demonstrated that the correlation between PET images corrected with aligned and shifted CT becomes poorer with increasing manual misregistration especially in the left, right, feet, and head directions. Some regions of the myocardial wall showed artificially low uptake values in case of large manual misregistrations between PET and CT data owing to wrong projection of lung tissue in CT data on the myocardial wall of the corresponding PET data and the large difference between attenuation factor at 511 keV for cardiac and lung tissues (0.1 cm-1 vs. 0.02 cm-1) [22]. This might induce hypo-perfusion in some cardiac territories leading to clinical misinterpretation [20]. In clinical studies, with increasing manual misregistration, the misalignment had severe influence in the motion toward the head and feet directions. This artefact was not so intense in the motionless experimental phantom.

The misalignment between PET and CT data produced significant quantitative artefacts in myocardial uptake values for movements in the posterior direction in comparison with that of the anterior direction. This effect was increasingly amplified with increasing levels of misalignment, as manifested by the decreasing correlation coefficients and slopes of the regression lines. Only slight variations in uptake values were observed for small (e.g. 5mm) movements in the anterior direction. In this direction, the strongest impact was observed for the lateroinferior, inferolateral and inferoseptal segments of the

myocardial wall with increasing global misalignments. Comparatively, in the posterior direction, the highest variations were observed at the anteroseptal, anterolateral and inferolateral regions of the myocardial wall. Our results indicate that the misalignment between CT and PET data had considerable influence in head, feet, left and right directions in comparison to the anteriorand posterior directions. We found that even 5 mm misalignments in the right, feet and head directions can cause considerable errors in myocardial wall activity quantification.

For movements in the head and feet directions, significant uptake variations were observed in all segments of the myocardial wall even in small (e.g. 5 mm) drifts. With increasing movements, the lateral wall was the most impacted segment (for head movements), while the anterior, septal and apical segments showed greatest variations for feet movements.

In agreement with findings by Martinez-Moller et al. [22], we observed that misalignments in the head and feet directions could produce significant artificial uptake in the myocardial wall of PET images. Mean absolute percentage differences in uptake value as high as 23.6±9.9% in the anteroseptal wall (for feet movement) and 33.0±9.7% in the lateroinferior wall (for head movement) were obtained. With 10 mm misalignment in the left direction, all segments of the myocardial wall were susceptible to produce noticeable errors, though this effect was amplified in the lateral wall. For movements in the right direction, the anterior and lateral walls were most affected.

Our regional analysis of different movements revealed that changes in apparent activity concentration in the myocardium were not uniform in all segments, though misalignments can lead to errors in all segments of the myocardial wall. The impact of global translations between CT and PET data on apparent activity concentration of the myocardium in PET images were most severe for movements in the right, feet, head, left, posterior and anterior directions (in descending order).

5. Conclusions

We analyzed the effect of varying global misalignments between transmission and emission data in the context of myocardial PET imaging using experimental and clinical studies. The misalignment can lead to non-uniform uptake in the myocardium. In particular, the anterior, lateral and septal wall segments were susceptible to increasing changes proportionally to the magnitude of misalignment. In descending order, misalignment artefacts varied in intensity depending on whether movements occurred in the right, feet, head, left, posterior and anterior directions. For a small shift (5-mm) of the CT image, errors in interpretation of PET images could occur for movements in the right, feet and head directions and the errors can be more significant with increasing drifts. Only movements as high as 10mm in magnitude in the left, posterior and anterior directions produced noticeable errors in tracer uptake value.

Acknowledgment

This work was supported by Tehran University of Medical Sciences under grant No. 12001, and Masih Daneshvari Hospital and Shahid Beheshti University of Medical Sciences and the Swiss National Science Foundation under grants SNSF 31003A-149957.

References

[1] M. F. Di Carli, S. Dorbala, J. Meserve, G. El Fakhri, A. Sitek, and S. C. Moore, "Clinical myocardial perfusion PET/CT," Journal of Nuclear Medicine, vol. 48, pp. 783-793, 2007.

[2] P. Knaapen, S. De Haan, O. Hoekstra, R. Halbmeijer, Y. Appelman, J. Groothuis, et al., "Cardiac PET-CT: advanced hybrid imaging for the detection of coronary artery disease," Netherlands Heart Journal, vol. 18, pp. 90-98, 2010.

[3] S. Kajander, H. Ukkonen, H. Sipilä, M. Teräs, and J. Knuuti, "Low radiation dose imaging of myocardial perfusion and coronary angiography with a hybrid PET/CT scanner," Clinical physiology and functional imaging, vol. 29, pp. 81-88, 2009.

[4] S. V. Nesterov, C. Han, M. Mäki, S. Kajander, A. G. Naum, H. Helenius, et al., "Myocardial perfusion quantitation with 15O-labelled water PET: high reproducibility of the new cardiac analysis software (Carimas™)," European journal of nuclear medicine and molecular imaging, vol. 36, pp. 1594-1602, 2009.

[5] M. Hacker, "Cardiac PET-CT and CT Angiography," Current Cardiovascular Imaging Reports, vol. 6, pp. 191-196, 2013.

[6] G. V. Heller, D. Calnon, and S. Dorbala, "Recent advances in cardiac PET and PET/CT myocardial perfusion imaging," Journal of nuclear cardiology, vol. 16, pp. 962-969, 2009.

[7] P. Ghafarian, S. M. R. Aghamiri, M. R. Ay, B. Fallahi, A. Rahmim, T. H. Schindler, et al., "Coronary calcium score scan-based attenuation correction in cardiovascular PET imaging," Nuclear medicine communications, vol. 31, pp. 780-787, 2010.

[8] H. Zaidi, R. Nkoulou, S. Bond, A. Baskin, T. Schindler, O. Ratib, et al., "Computed tomography calcium score scan for

attenuation correction of N-13 ammonia cardiac positron emission tomography: effect of respiratory phase and registration method," The international journal of cardiovascular imaging, vol. 29, pp. 1351-1360, 2013.

[9] P. Ghafarian, S. Aghamiri, M. R. Ay, A. Rahmim, T. H. Schindler, O. Ratib, et al., "Is metal artefact reduction mandatory in cardiac PET/CT imaging in the presence of pacemaker and implantable cardioverter defibrillator leads?," European journal of nuclear medicine and molecular imaging, vol. 38, pp. 252-262, 2011.

[10] M. R. Ay, A. Mehranian, M. Abdoli, P. Ghafarian, and H. Zaidi, "Qualitative and quantitative assessment of metal artifacts arising from implantable cardiac pacing devices in oncological PET/CT studies: A phantom study," Molecular Imaging and Biology, vol. 13, pp. 1077-1087, 2011.

[11] R. Nakazato, D. Dey, E. Alexánderson, A. Meave, M. Jiménez, E. Romero, et al., "Automatic alignment of myocardial perfusion PET and 64-slice coronary CT angiography on hybrid PET/CT," Journal of Nuclear Cardiology, vol. 19, pp. 482-491, 2012.

[12] K. L. Gould, T. Pan, C. Loghin, N. P. Johnson, A. Guha, and S. Sdringola, "Frequent diagnostic errors in cardiac PET/CT due to misregistration of CT attenuation and emission PET images: a definitive analysis of causes, consequences, and corrections," Journal of Nuclear Medicine, vol. 48, pp. 1112-1121, 2007.

[13] A. M. Alessio, P. E. Kinahan, K. M. Champley, and J. H. Caldwell, "Attenuation-emission alignment in cardiac PET/CT based on consistency conditions," Medical physics, vol. 37, pp. 1191-1200, 2010.

[14] A. Rahmim, O. Rousset, and H. Zaidi, "Strategies for motion tracking and correction in PET," PET Clinics, vol. 2, pp. 251-266, 2007.

[15] R. G. Wells, T. D. Ruddy, R. A. DeKemp, J. N. DaSilva, and R. S. Beanlands, "Single-phase CT aligned to gated PET for respiratory motion correction in cardiac PET/CT," Journal of Nuclear Medicine, vol. 51, pp. 1182-1190, 2010.

[16] T. Pan, O. Mawlawi, S. A. Nehmeh, Y. E. Erdi, D. Luo, H. H. Liu, et al., "Attenuation correction of PET images with respiration-averaged CT images in PET/CT," Journal of Nuclear Medicine, vol. 46, pp. 1481-1487, 2005.

[17] A. M. Alessio, S. Kohlmyer, K. Branch, G. Chen, J. Caldwell, and P. Kinahan, "Cine CT for attenuation correction in cardiac PET/CT," Journal of Nuclear Medicine, vol. 48, pp. 794-801, 2007.

[18] K. R. Zasadny and R. L. Wahl, "Standardized uptake values of normal tissues at PET with 2-[fluorine-18]-fluoro-2-deoxy-D-glucose: variations with body weight and a method for correction," Radiology, vol. 189, pp. 847-850, 1993.

[19] A. M. Loening and S. S. Gambhir, "AMIDE: a free software tool for multimodality medical image analysis," Molecular imaging, vol. 2, pp. 131-137, 2003.

[20] K. Khurshid, R. J. McGough, and K. Berger, "Automated cardiac motion compensation in PET/CT for accurate reconstruction of PET myocardial perfusion images," Physics in medicine and biology, vol. 53, p. 5705, 2008.

[21] T. DesJardins, Cardiopulmonary anatomy and physiology: Essentials of Respiratory Care. New York: Delmar Thomson Learning Inc, 2002.

[22] A. Martinez-Möller, M. Souvatzoglou, N. Navab, M. Schwaiger, and S. G. Nekolla, "Artifacts from misaligned CT in cardiac perfusion PET/CT studies: frequency, effects, and potential solutions," Journal of Nuclear Medicine, vol. 48, pp. 188-193, 2007.